NASA

Technical Memorandum 78043

Observations of Solar Active Regions and Solar Flares by OSO-7

W. M. Neupert

DECEMBER 1977

National Aeronautics and Space Administration

Goddard Space Flight Center
Greenbelt, Maryland 20771

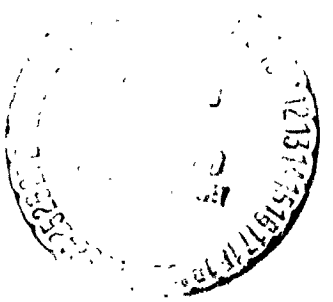

BIBLIOGRAPHIC DATA SHEET

1. Repc · No.	2. Government Accession No.	3. Recipient's Catalog No.
TM 78043		

4. Title and Subtitle	5. Report Date
Observations of Solar Active Regions and Solar Flares by OSO-7	December 1977
	6. Performing Organization Code: 682
7. Author(s): W. M. Neupert	8. Performing Organization Report No.
9. Performing Organization Name and Address: NASA-Goddard Space Flight Center, Greenbelt, Maryland 20771	10. Work Unit No.
	11. Contract or Grant No.
	13. Type of Report and Period Covered
12. Sponsoring Agency Name and Address	
	14. Sponsoring Agency Code

15. Supplementary Notes

16. Abstract

This review paper discusses contributions made to the physics of coronal active regions and flares by the GSFC Extreme Ultraviolet and Soft X-Ray Spectroheliograph on OSO-7. Coronal structures above active regions are discussed from the point of view of their morphology and physical properties, including their relationship to photospheric and coronal magnetic fields. OSO-7 also recorded flares with sufficient spatial (20 arc sec) and temporal resolution (one minute) to record, in some instances for the first time, the extreme ultraviolet and soft X-ray emission associated with such chromospheric phenomena as filament activation and the emergence of satellite sunspots. Flare phenomena are reviewed in terms of the several stages of evolution typically associated with the event - the pre-flare buildup, the impulsive phase and the post-maximum phase.

17. Key Words (Selected by Author(s))	18. Distribution Statement
solar, flares, solar corona	

19. Security Classif. (of this report)	20. Security Classif. (of this page)	21. No. of Pages	22. Price*
Unclassified	Unclassified		

*For sale by the National Technical Information Service, Springfield, Virginia 22151.

GSFC 25-44 (10/77)

OBSERVATIONS OF SOLAR ACTIVE REGIONS AND SOLAR FLARES BY OSO-7

W. M. Neupert

Laboratory for Astronomy and Solar Physics
NASA-Goddard Space Flight Center
Greenbelt, Maryland 20771

Invited paper presented at the OSO-8 Workshop, Boulder, Colo., Nov. 8, 1977.

OBSERVATIONS OF SOLAR ACTIVE REGIONS AND SOLAR FLARES BY OSO-7

W. M. Neupert
Laboratory for Astronomy and Solar Physics
NASA-Goddard Space Flight Center

Abstract. This review paper discusses contributions made to the physics of coronal active regions and flares by the GSFC Extreme Ultraviolet and Soft X-Ray Spectroheliograph on OSO-7. Coronal structures above active regions are discussed from the point of view of their morphology and physical properties, including their relationship to photospheric and coronal magnetic fields. OSO-7 also recorded flares with sufficient spatial (20 arc sec) and temporal resolution (one minute) to record, in some instances for the first time, the extreme ultraviolet and soft X-ray emission associated with such chromospheric phenomena as filament activation and the emergence of satellite sunspots. Flare phenomena are reviewed in terms of the several stages of evolution typically associated with the event - the pre-flare buildup, the impulsive phase and the post-maximum phase.

I. INTRODUCTION

The versatility of the sun's extreme ultraviolet and soft X-ray spectrum as a tool for coronal research is by now well appreciated, with many contributions being made by this OSO series of satellites, the ATM Skylab mission and NASA's ongoing rocket program. In this paper I would like to discuss some of the observations and results obtained with the OSO-7 extreme ultraviolet (EUV) and soft X-ray spectroheliograph to the topics of solar activity and solar flares. The wavelength range that was covered - 1.8Å - 15Å, 120Å - 400Å and Hα at 6563Å cover emission lines produced over a wide range of electron temperature in the solar transition region and corona. Spatial resolution was 20 arc sec. The instrument was designed to provide four simultaneous spectroheliograms - two in the soft X-ray region and two in the EUV (with a limited substitution of Hα possible). Further automatic operational sequences through six X-ray channels and/or four EUV channels were possible so that a wide range of plasma temperatures could be obtained at the expense of temporal resolutions.

II. OBSERVATIONS OF ACTIVE REGIONS

Observations made from rockets and satellites at soft X-ray and EUV wavelengths have clearly shown the magnetically confined systems of coronal loops which connect regions of opposite magnetic polarity, either in the same active region or in neighboring regions (Vaiana et al. 1968, Krieger et al. 1971, Tousey et al. 1973). From spectroscopic observations made even earlier both from the ground (see Billings, 1966 for a review of the observational material) and from space (Widing and Sandlin, 1968, Noyes et al. 1970) it was evident that the enhanced emission associated with active regions could be attributed to increases in both electron temperature and density as compared to the "quiet" corona.

As the phototype of coronal active regions observed by OSO-7 I would like to consider a magnetically bipolar region far removed from other regions of activity. Observations of this region were made over a two week period as it crossed the disk in January 1972 (Neupert, Nakagawa and Rust, 1975). During this period, it was the site of flare activity (to be addressed later) and ultimately evolved into a magnetically complex region as it approached the west limb of the sun. Its location and appearance at central meridian passage is shown, both in Hα and two EUV observations on January 19, 1972 in Fig. 1. The magnetic neutral line of zero longitudinal field runs generally in an east-west direction and separates magnetic fields of opposite polarity. While the regions of greatest emission at 304Å (He II) correspond well to the Hα plage, emission from lines at transition region temperatures (500,000K - 1.0 x 10^6K) such as those of Mg VIII is more extended, showing outlying bright patches that may represent the footpoints of high loop systems. At high electron temperatures, e.g., 2.3 x 10^6K at which the contribution function for Fe XVI peaks, the emitting region is markedly simpler and is localized in one region lying between areas of opposite magnetic polarity. The simplest geometry which satifies these high temperature observations is in fact a set of rather flat magnetic arches, hottest at their tops and with their footpoints in the brightest chromospheric plage. Such a simple picture becomes immediately more complex when we examine spectroheliograms representing plasma at intermediate temperatures i.e. 1.0 - 2.0 x 10^6K (Fig. 2). From these we find that the orientation of the apparent arches of emission crossing the neutral line depends upon the ion being observed. A possible model, based on the data and on computer-generated force-free magnetic fields (Nakada and Raadu, 1972), is a set of nested arched defined by force-free magnetic fields whose orientations, relative to magnetic neutral line, change with increasing electron temperature. From Fig. 2 we infer that both positive and negative values of the current-proportional parameter α may be present, implying that opposing currents may be possible in neighboring coronal loops or arches. A similar conclusion has been obtained by Levine (1976) from an examination of ATM data. A present limitation in such analyses is that the calculation of the coronal field must be performed with a constant value of α for the entire region. This simplification obviously does not correspond to reality.

Recognizing that ambiguities and uncertainties exist because of the limited spatial resolution that was available, we can still present some qualitative conclusions concerning the rather flat-arch high temperature coronal features:

1. Active region structures occur as arches or loops between regions of opposite magnetic polarity generally in a geometry that is consistent with the presence of electric currents. There is some evidence in the OSO-7 data that the top of an arch or loop is its hottest point. Any single loop or arch is

nearly isothermal except at its footpoints. Typical characteristics for two cases that have been analyzed are given in Table 1 (Neupert et al., 1975; Levine and Withbroe, 1976).

2. Radiative losses are greater than conductive losses to the chromosphere in the one case we have examined in detail. Such losses must be balanced by a energy input to maintain the temperature of the coronal structure. If this is to be injected through the footpoints, then about 1.5 x 10 erg cm^{-2} s^{-1} are required to maintain the hottest loops. Alternatively, dissipation of magnetic fields, if it occurs rather uniformly throughout the length of the arch, is another possible energy source (Tucker, 1973). In any event, the lifetime of the system, if the energy input is removed, is of the order of an hour or two Such an occurrence has been reported by Levine and Withbroe (1976).

TABLE I. Typical Properties of Active Region Coronal Arches

	OSO-7 (Neupert et al., 1975)	ATM (Levine and Withbroe, 1972)
Ion	Fe XV, Fe XVI	Mg X
Height	20-40 x 10^3 km	$\approx$ 30 x 10^3 km
Diameter	20 x 10^3 km	14 x 10^3 km
T_e max	2.6 x 10^3K	1.4 x 10^6K
n_e	6.7 x 10^9 cm^{-3}	1.8 x 10^9 cm^{-3}
Pressure ($3n_e kT$)	7.2 dyn cm^{-2}	0.8 dyn cm^{-2}
Energy dissipation	2.3 x 10^{-3} erg cm^{-3} s^{-1}	2.4 x 10^{-4} erg cm^{-3} s^{-1}
$\tau_{cooling}$ (radiative loss)	3.5 x 10^3 s	1 x 10^3 s

III. OBSERVATIONS OF SOLAR FLARES

Let us start by addressing the question of the location of the initial phase of a typical active region flare - in the corona? - or in the chromosphere? - or somewhere in between, recognizing that our standard concepts of these terms may not be appropriate in most highly structured centers of activity. Our answer from the OSO-7 data must be a guarded one because of the limited spatial resolution. It appears however, that the flare does not begin in the bright coronal features of active regions. If the event begins in the corona i.e. in regions with $T_e > 1.5 \times 10^6$K,

that location must be of very low initial brightness and of low contrast with its surroundings. As an illustration of this statement, Fig. 3 shows the coronal (and chromospheric) emission in several lines prior to an event on August 2, 1972 and the subsequent appearance of a flare. Note that the flare does not coincide with any definite coronal feature prior to the event. Furthermore, there appears no way in which the pre-flare emission Fe XIV line emission (5% of the flare maximum) at the site of the eventual flare could account for the eventual flare emission. A compression of the Fe XIV emitting region could in fact produce the emission measure we record at higher temperature during the flare, but then the Fe XIV emission would have to vanish. In fact, we recorded enhanced emission measures (above that inferred for Fe XIV at the flare site prior to the flare) at all temperatures up to 30×10^6 K. Generally, we can state that the high temperature coronal emission of Fe XV and Fe XVI associated with active region loops is enhanced after the beginning of a flare - primarily after the impulsive phase is ended - but does not give evidence of enhanced emission during the impulsive phase of a flare.

If we do not see the flare beginning in the high-temperature corona, then where does it first radiate in the extreme ultraviolet? Our evidence, based on those instances for which our spatial resolution is adequate to draw conclusions, is that the EUV emission from transition region lines He II up through those emission lines formed at 1×10^6K (or somewhat above) is enhanced at the same time and at the same location where an Hα point brightening signals the beginning of the impulsive phase of a flare event. Such emission is very transitory and can be associated with the impulsive phase of the flares evolution as originally pointed out by Kane and Donnelly (1971). An impulsive EUV component appears to be present for a wide range of time scales of flare phenomena, i.e., not only in very rapidly developing events but also in slowly evolving flares. As an example of the former case, Fig. 4 shows the impulsive development of a flare on August 2, 1972. In this case, the low-temperature EUV component reached maximum in about one minute (coincident with the hard X-ray emission recorded by the UCSD instrument), followed one minute later by maximum emission in the highest temperature thermal plasma ($\sim$ 20-30 $\times 10^6$K recorded in emission of Fe XXV and Fe XXVI) and two minutes later by a maximum of $\sim 10 \times 10^6$K plasma (Fe XVII). Even with such a rapid evolution, the emission occurs in a well defined loop system bridging the neutral line of the photosphere longitudinal magnetic field with the highest temperature plasma apparently radiating from a different loop than the lower (but still 10×10^6K) temperature component.

A second example of the impulsive component is shown in Fig. 5 where it is recorded in an emission line of Fe XI at 180.5A (Thomas, 1975). Note that no impulsive component is recorded in Hα simultaneously by the instrument although the initial Fe XI emission seems to be located close to the initial site of Hα emission (Fig. 6). This site must also be the location of an explosive phenomenon for we record ejecta in Fe XI originating there and moving toward the center of the lower margin of

the field of view at a rate of about 600 km/s normal to the line of sight.

Finally we consider a slow-rise flare, on January 19, 1972 which was sufficiently extended spatially that we could record the temporal and spatial sequence of events occurring in the initial phase of the flare's development. This flare, recorded simultaneously by OSO-7 and Sacramento Peak Observatory by David Rust (Rust et al. 1975) was preceded by the activation (an apparent untwisting) of a dark filament located along the magnetic neutral line (Fig. 7). The flare itself began with the appearance near the center of the filament of a bright Hα knot at about 1634 UT. This was identified as the trigger phase (located at point "A") and was accompanied by a burst in the EUV lines of Mg VIII and Mg IX at 315Å and 368Å respectively (Fig. 8). As this first bright EUV point faded, a second, labeled "B" at the southern footpoint of the erupting filament and on the opposite side of the neutral line appeared, followed eventually by a third "C" near the northern footpoint. The concurrent soft X-ray (Fig. 9) observations showed no similar impulsive event with the first Hα brightening but did show a momentary peak, superimposed on a gradually rising level, associated with the second Hα brightening. The soft X-ray emission distributed along a line connecting "A", "B", and "C" continued to increase monotonically as the filament erupted. The velocity of eruption observed off-band at Hα at the center of the filament was at least 100 km/s outward while the ends of the filament displayed a downward motion. Similar outward velocities (as well as turbulent components) have been recorded in the Fe XXIV emission line at 244Å by the NRL ATM 5082A instrument on Skylab so there is strong evidence that the matter that eventually forms the hot X-ray emitting flare plasma is identical to or is at least closely associated with the activated filament.

An examination of sunspot photographs and magnetograms taken during the event revealed that two sunspots emerged during the event and that, in fact, new flux was emerging through the photosphere and chromosphere immediately adjacent to the eruptive filament and at the point where the flare started. Force-free field modeling (Nakagawa and Raadu, 1972) of the region indicated that sufficient energy, about 10^{32} ergs, was available in the magnetic field to power a 1B flare. While many questions concerning the actual source of energy required to drive this event go unanswered, the close spatial coincidence of new emerging magnetic flux (10^{19} Mx Hz^{-1}) with initial Hα and transition region brightenings lends support to the theory of Priest and Heyvaerts (1974) in which a plasma instability could start where emergent flux intersects overlying fields.

It is worthwhile to emphasize that impulsive brightenings in transition region and lower temperature coronal lines are present in all three events and others that we have recorded, so they appear to be a very common characteristic of active region flares. Furthermore, when more than one bright point is distinguished in an event, the brightenings are sequential and not coincident.

We now go on to discuss the maximum and post-maximum phases of typical events. OSO-7 observed, as did also the ATM instruments with much better spatial resolution (Cheng and Widing, 1975; Kahler, Krieger and Vaiana, 1975; Brueckner, 1976), the formation of a high temperature ($2 - 20 \times 10^6$K) plasma in magnetically structured arches crossing the neutral line. Such arches have remarkable stability in time, although observations of line broadening imply that the material contained within them in a turbulent state (ion velocities of 60-120 km s^{-1})(Brueckner, 1976). OSO-7 observations suggest that these flare arches, confined by coronal magnetic fields which are probably already present prior to the flare, have a nested configuration, with cooler ($2 - 10 \times 10^6$K) arches nested within hotter ($1 - 2 \times 10^7$K) arches. Data from the August 2 event (Fig. 9) show such a spatial separation of the cooler (Mg XI) and hotter (Fe XXV) components. On the other hand, the January 19, 1972 event occurred near the meridian and no spatial separation was detected.

A more striking example of the loop-like structure of X-ray emission was observed during the post-maximum phase of a limb flare on Feb. 9, 1972. Fig. 10 begins with observations taken at 0855 UT as a bright area in the lower right corner of the He II data frame was fading. This area corresponded to the location of an unconfirmed Hα subflare (importance-F) which had begun at 0820 and ended at 0850 (as observed at Carnarvon, Australia). We observed a low (maximum height of 8800 km) arch in Fe XVI and an even higher arch (maximum height of 40,000 km) in soft X-rays. The rate of decrease of this soft X-ray emission agrees with that recorded by the Solrad satellite during this event. Later in time a second He II bright point (not reported as a flare) appeared at distant footpoint of these high temperature arches and, even later, at the end of the daylit portion of the OSO orbit, a third region near the original flare began to brighten. Inasmuch as the Fe XVI emission originates in a temperature range intermediate to that of the soft X-ray emission and that of the chromospheric emission, we would expect to see the Fe XVI defining the legs of the arch whose top is a copious emitter of soft X-rays. This may be the case on the right hand side where the Fe XVI emission is the greatest. However on the left hand side, no evident relation exists between the Fe XVI and soft X-ray emission. Possibly some restriction or pinching of the high temperature arch is present near this one footpoint.

The complex spatial relations of flare emissions are again demonstrated in a dramatic way through observations of this same general region on February 9 following a flare behind the east limb of the sun which produced a system of large post-flare loops (Fig. 11). OSO-7 observed these loops in the transition lines of Mg VIII and Mg IX in which they were comparable to groundbased Hα data (although the observations were not exactly coincident in time)(Chapman, 1977). Such features are usually attributed to an arcade of arches seen end-on. However, at higher coronal temperatures (recorded in Fe XVI and soft X-ray emission) the spatial distribution of the radiation changed dramatically, becoming much more triangular in general outline with increasing T_e and having a region of enhanced emission at the apex of the triangle. It seems clear that the apex of

the X-ray emission extends higher above the limb than does the EUV emission. If, in fact, the structures that we recorded at these three wavelengths (and temperatures) are spatially related, it may be that the high lying X-ray emission represents hot plasma which, as it cools, condenses into the tops of the loops recorded in Mg VIII and drains downward through them to the chromosphere. Such a scenario had already been proposed (see Billings, 1966 for a review of this topic) on the basis of Ca XV (yellow line) observations of knots of hot material at the tops of the post-flare loops. The spatial distribution of Fe XVI is consistent with this interpretation. Furthermore, the observations demonstrate that there exists an even hotter, higher region emitting in X-rays. This region is evidently also contained by a magnetic field, and its shape reminds one of the Y shaped neutral point and neutral sheet concepts of solar flares discussed by Sweet (1958), Sturrock (1968) and others. We can find no evidence that the hot plasma originates there. However, R. Chapman (1977), who has analyzed this event, finds that energy must be continually supplied in order to maintain the X-ray emission over a period of nearly 2 days. Vorpahl (1975) has analyzed a similar event recorded by ATM and also finds that energy and possibly new material must be added to the X-ray loop system as it evolves. Two analyses of flare loop structures (Rust et. al., 1975; Cheng, 1977) are given in Table II.

Table II. Typical Properties of Flare Loops

	OSO-7 (Rust et al., 1975)	ATM (Cheng, 1977)
Ion	Fe XXV	Fe XXIV, Fe XXIII
Height	35×10^3 km	$\approx 7 \times 10^3$ km
Diameter	$\approx 3.5 \times 10^3$ km	1.5×10^3 km
T_e max	30×10^6 K	14×10^6 K
n_e	$\gtrsim 1.5 \times 10^{10}$ cm^{-3}	$\approx 1 \times 10^{11}$ cm^{-3}
Pressure ($3n_e kT$)	$\approx$ 180 dyn cm^{-2}	$\approx$ 580 dyn cm^{-2}
Energy dissipation	1-2 erg cm^{-3} s^{-1}	7 erg cm^{-3} sec^{-1}
$\tau_{cooling}$ (conduction)	$\approx$ 100 sec	10-100 sec

The preceding discussion of active region flares recorded by OSO-7 can be summarized in a number of main points:

1. No evidence has been found that material at coronal temperature residing in the low corona prior to an event is the source of matter for the hot thermal plasma produced during the event. Material at lower i.e. chromospheric temperature, such as a filament in the low corona, is a strong candidate for the eventual flare plasma, however. Activation of such a filament prior to the flare may be accompanied by a low level of soft X-ray emission.

2. An impulsive spike of emission at transition region temperatures, possibly up to 1.5×10^6K, is a common occurrence and can be spatially related to the first Hα brightenings of the flare. We associate this first flare brightening with the trigger of the flare phenomenon. In one event this brightening is located near a rapidly emerging region of magnetic flux beneath an existing filament. Instabilities during magnetic field line reconnection, as discussed by Spicer (1976), can lead to a release of magnetic energy residing in any force-free magnetic field configurations. As a result, electrons are accelerated to high energies. Their energy losses, produced through interactions with the solar plasma and magnetic fields, produce hard X-ray bursts, microwave emission and, sometimes, white light photospheric emission coincident with the impulsive EUV emission. Subsequent to the initial EUV brightening, one or more other locations in the flaring region may display short-lived brightenings. However, no instances of simultaneous brightening of two spatially separated points have been recorded. Such simultaneous effects would be expected if the initiation of the flare occurred at the top of a coronal loop system and traveled concurrently to the chromospheric footpoints of the coronal loop (Sturrock, 1968).

3. The impulsive phase is accompanied by a rapid rise in the soft X-ray emission as a high temperature plasma is formed. Its apparent electron temperature, derived either from observations of the thermal continuum (Datlowe, 1974) or line emission of Fe XXV (Phillips, Neupert and Thomas, 1974), reaches a maximum as the impulsive phase terminates. In one event recorded this emission can be attributed to ionization of material in a dark filament. Similar instances of X-ray emission originating in disappearing filaments have been recorded by ATM (Webb, Krieger and Rust, 1976; Sheeley et. al., 1977). Thus, the heating and ionization of material originally at chromospheric or near-chromospheric temperatures does appear to explain the appearance of the hot flare plasma (Neupert, 1968, Hiryama, 1974). Such ionization occurs over an extended region of the filament (in contrast to the point-like location of the initial trigger phenomenon) and suggests that a second type of energy conversion, again possibly a plasma instability but in this case associated with turbulent magnetic fields, rather than the ordered fields present when the flare is triggered, is present (Spicer 1976). The hot plasma, although exhibiting turbulent velocities, is localized in stable coronal

loop systems. Further brightenings in transition region lines may occur during the build-up of the hot thermal plasma and may be the consequence of heat conduction from that plasma into the chromosphere (Somov and Syrovatskii, 1974; Somov, 1975). In some instances, mass ejections originating from the corona - chromosphere interface are observed in emission lines emitted by the same ions which radiate during the impulsive phase, i.e. at $T_e \lesssim 1.5 \times 10^6$K. This mass loss may represent a portion of an erupting filament or may represent chromospheric material, ejected into an open magnetic configuration. This ejection originates at or near chromosphere heights, not at the tops of coronal loops, implying that an explosive heating of plasma originates in the high chromosphere or transition region.

REFERENCES

Billings, D. E.: 1966, A Guide to the Solar Corona, Academic Press, New York

Brueckner, G.: 1976, Phil. Trans. R. Soc. Lond. A281, 443.

Chapman, R. D.: 1977, Private Communication.

Cheng, C. C.: 1977, NRL Skylab/ATM Preprint "Evolution of the High-Temperature Plasma in the 15 June 1973 Flare".

Cheng, C. C. and Widing, K. G.: 1975, Astrophys. J. 735.

Datlowe, D. W., Hudson, H. S., and Peterson, L. E.: 1974, Solar Phys. 35, 193.

Hirayama, T.: 1974, Solar Phys. 34, 323.

Kahler, S. W., Krieger, A. S., and Vaiana, G. S.: 1975, Astrophys. J. (Letters) 199, L57.

Kane, S. R. and Donnelly, R. F.: 1971, Astrophys. J. 164, 151.

Krieger, A. S., Vaiana, G. S., and Van Speybroeck, L. : 1971 in R. Howard (ed.); "Solar Magnetic Fields", IAU Symp. 43, 397.

Levine, R. H.: 1976, Solar Phys. 46, 159.

Nakagawa, Y., and Raadu, M. A.: 1972, Solar Physics 25, 127.

Neupert, W. M.: 1968, Astrophys. J. 153, L59.

Neupert, W. M., Nakagawa, Y., and Rust, D. M.: 1975, Solar Physics 43, 359.

Noyes, R. W., Withbroe, G. L., and Kirschner, R. P.: 1970, Solar Physics 11, 388.

Phillips, K. J. H., Neupert, W. M., and Thomas, R. J.: 1974, Solar Phys. 36,

Priest, E. R. and Heyvaerts, J.: 1974, Solar Phys. 36, 433.

Sheeley, N. R., Bohlin, J. D., Brueckner, G. E., Purcell, S. D., Scherrer, V. E., and Tousey, R.: 1977, NRL Skylab/ATM Preprint "Coronal Changes Associated with a Disappearing Filament".

Spicer, D. S.: 1976, NRL Skylab/ATM Preprint "The Thermal and Non-Thermal Flare: A Result of Non-Linear Threshold Phenomena during Magnetic Field Line Reconnections".

Somov, B. V.: 1975, Solar Phys. 42, 235.

Somov, B. V. and Syrovatskii, S. I.: 1974, Solar Phys. 39, 415.

Sturrock, P. A.: 1968, in K. O. Kiepenheuer (ed.), 'Structure and Development of Solar Active Regions', I.A.U. Symp. 35, 471.

Sweet, P. A.: 1958, in B. Lehnert (ed.), "Electromagnetic Phenomena in Cosmical Physics", Cambridge University Press, p. 123.

Thomas, R. J.: 1975 in S. Kane (ed.), "Solar Gamma-, X-, and EUV Radiation", I.A.U. Symp., 25.

Tousey, R., Bartoe, J.-D. F., Bohlin, J. D., Brueckner, G. E., Purcell, J. D., Scherrer, V. E., Sheeley, Jr., N. R., Schmacher, R. J., and Vanhoosier, M. E.: 1973, Solar Phys. 33, 265.

Vaiana, G. S., Reidy, W. P., Zehnpfennig, T., Van Speybroeck, L., and Giaconni, R.: 1968, Science, 161, 564.

Vorpahl, J., Tandberg-Hanssen, E., and Smith, J. B., Jr.: 1977, Astrophys. J. 212, 550.

Webb, D. F., Krieger, A. S., and Rust, D. M.: 1976, Solar Phys. 48, 159.

Widing, K. G. and Sandlin, G. D.: 1968, Astrophys. J. 152, 545.

FIGURE CAPTIONS

Fig. 1. Observations of an active region on January 19, 1972, showing (a) the location of the active region on the solar disk, (b) isogauss contours of the longitudinal photospheric magnetic field as measured at Sacramento Peak Observatory at 1619 UT superimposed on Hα, (c) the corona in the radiation of Fe XVI(335.4Å) at 1614 UT and (d) the high transition region in the radiation of Mg VIII(315.0Å) (at the same time as (c)). Frames (b), (c), and (d) are all to the same spatial scale and cover that portion of the solar disk surrounded by the black rectangle in Frame (a). In (b), the solid and dashed contours represent areas of opposite polarity. The neutral line generally coincides with the dark filament through the region. The EUV isophotes in (c) and (d) are scaled in increments of 5% of the peak intensity recorded in each spectroheliogram.

Fig. 2. Comparison of calculated constant α force-free coronal magnetic fields, derived from the observed photospheric (longitudinal) field shown in Figure 1, with EUV emission from OSO-7. An arch of EUV emission crossing the neutral line is observed in each stage of ionization but the orientation of the emission (angle relative to the neutral line) as indicated by the dashed lines changes from one stage of ionization to the next. To match these orientations in the calculated magnetic field requires a change in the current-proportional parameter α, thus implying currents of differing magnitude and direction as a function of height in the lower corona.

Fig. 3. Spectroheliograms of solar emission prior to and during the impulsive phase of a flare. Intensity levels have been normalized so that the increment between two isophotes represents one-eighth of the maximum count (shown in the upper right corner found in that spectroheliogram. Note that only weak EUV and no measurable soft X-ray emission emanated from the site of the flare before the event began at 1838 UT.

Fig. 4. The intensity of the brightest point in the EUV flare of August 2, 1972, at two wavelengths: 2190Å and 294.9Å. Note the impulsive phase between 1838 and 1842 UT and the gradual phase after 1842 UT seen at both wavelengths.

Fig. 5. Time history of the peak intensity of a flare on 1972, February 13 observed by OSO-7 at three wavelengths in the visible (Hα), soft X-rays (Mg XI, XII), and EUV (Fe XI).

Fig. 6. Time sequence from left to right of OSO-7 spatial maps in a grey-scale representation for the flare shown in Figure 5. From top to bottom are maps 5' square in Hα, Fe XI, Mg XI-XII and Si XIII-XIV. The sequence on the left covers the impulsive phase at roughly one-minute intervals. The set on the right were all made at the peak of the gradual component. Dark markings in the center of some Fe XI maps are due to computer overflow and actually represent the very brightest location.

Fig. 7. Comparison of Hα, Mg VIII and soft X-ray observations prior to and during the flare of January 19. Points A, B, and C, the sites of successive EUV brightenings are indicated. Weak soft X-ray emission was observed in the region of the activating filament before the beginning of the event.

Fig. 8. EUV (Mg VIII at 315.0Å) (above), and soft X-ray (Mg XI, Mg XII and continuum at 7.95-9.51Å) (below), emission as a function of time for three locations (points A, B, and C on the previous figure). Maxima of Mg VIII emission were associated with the trigger phase of the flare (point A), with one end of the disrupting filament (point B), and with the rapid expansion of Hα emission (point C). Soft X-ray emission displayed a gradual rise throughout this interval of time except for a small additional enhancement at point B at 1638-1639 UT.

Fig. 9. Comparison of XUV spatial distribution during the post-impulsive phase of the flare with an off-band (Hα + 0.6Å) photograph made at the Lockheed Solar Observatory. The radiation at 294.9Å attributed to chromospheric emission coincides with the Hα brightening present at nearly the same time. Soft X-ray emission from Mg XI and Mg XII (b) and highly ionized iron (primarily Fe XXV) (c) localized in loop-like features extending across the neutral line of the longitudinal photospheric magnetic field (marked by a diagonal break in the Hα flare filament).

Fig. 10. Spectroheliograms made in the emission lines of He II, Fe XVI, and primarily) Si XIII and Si XIV during the post-maximum phase of a limb flare. The soft X-ray emission is situated in one or perhaps several loops extending to a maximum height of 40,000 km above the photospheric limb (indicated by the dashed lines).

Fig. 11. Spectroheliograms made in the emission lines of Mg XIII, Fe XVII and (primarily) Mg XI and Mg XII in the region of observed Hα loop prominences on the east limb of the sun on February 9, 1972. Enhanced X-ray emission is attributed to a long-lived event first recorded by Solrad 9 on February 8, 1972. No Hα flare was reported although presumed present behind the solar limb.

FIGURE 1

COMPARISON OF EUV EMISSION WITH CALCULATED FORCE-FREE MAGNETIC FIELDS

16:19 UT, Jan. 19, 1972

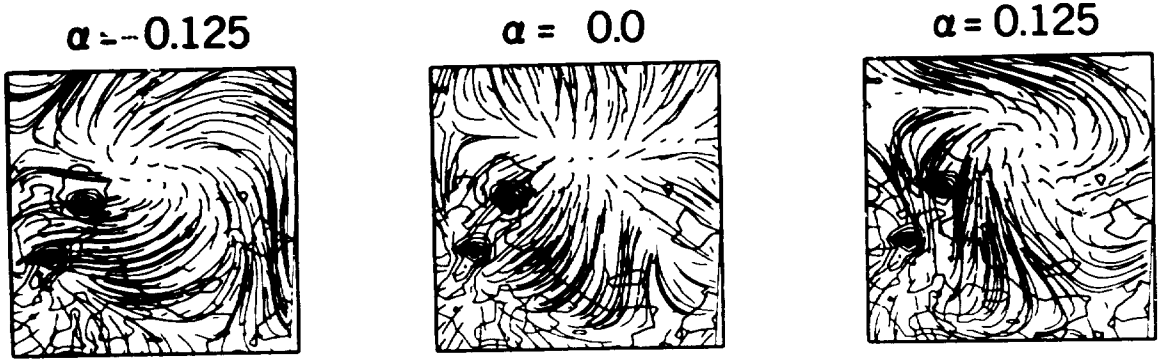

22:38 - 22:52 UT, Jan. 19, 1972

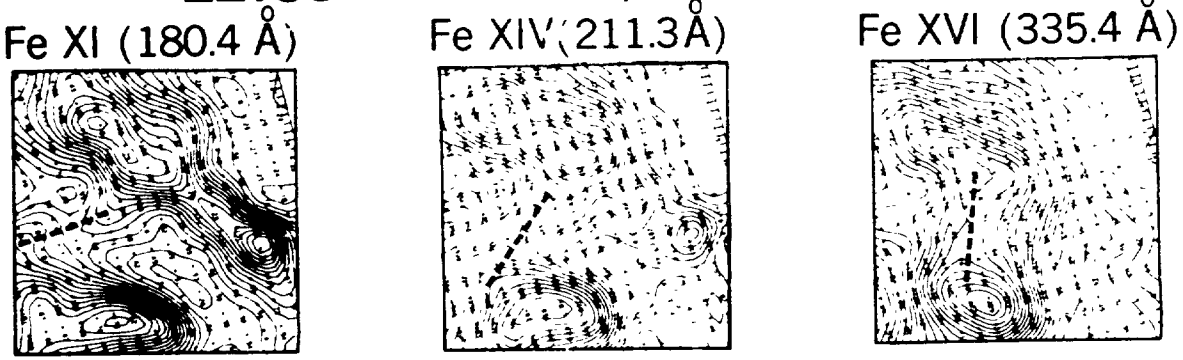

FIGURE 2

294.9Å (CHROMOSPHERIC RADIATION)

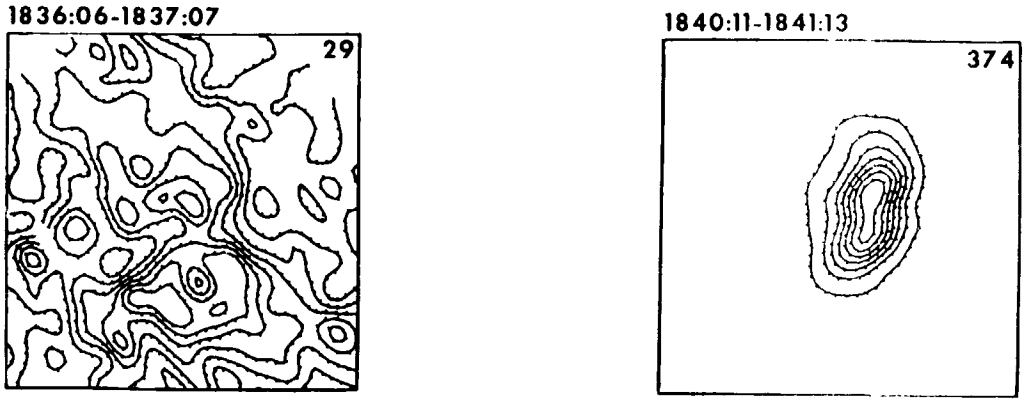

219.0Å (Fe XIV)

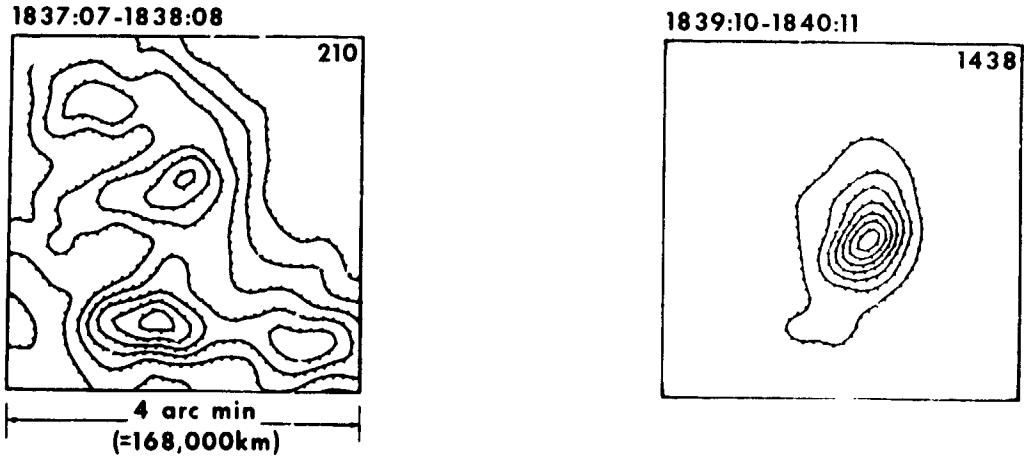

14.50-15.90Å (Fe XVII)

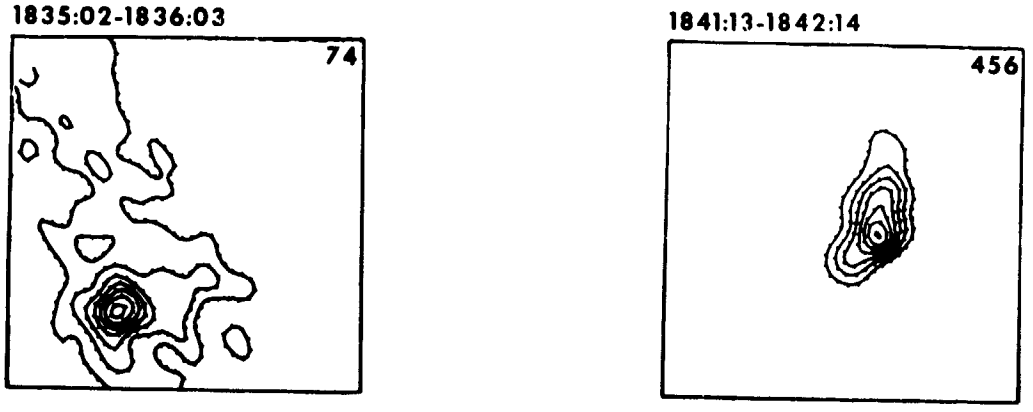

FIGURE 3

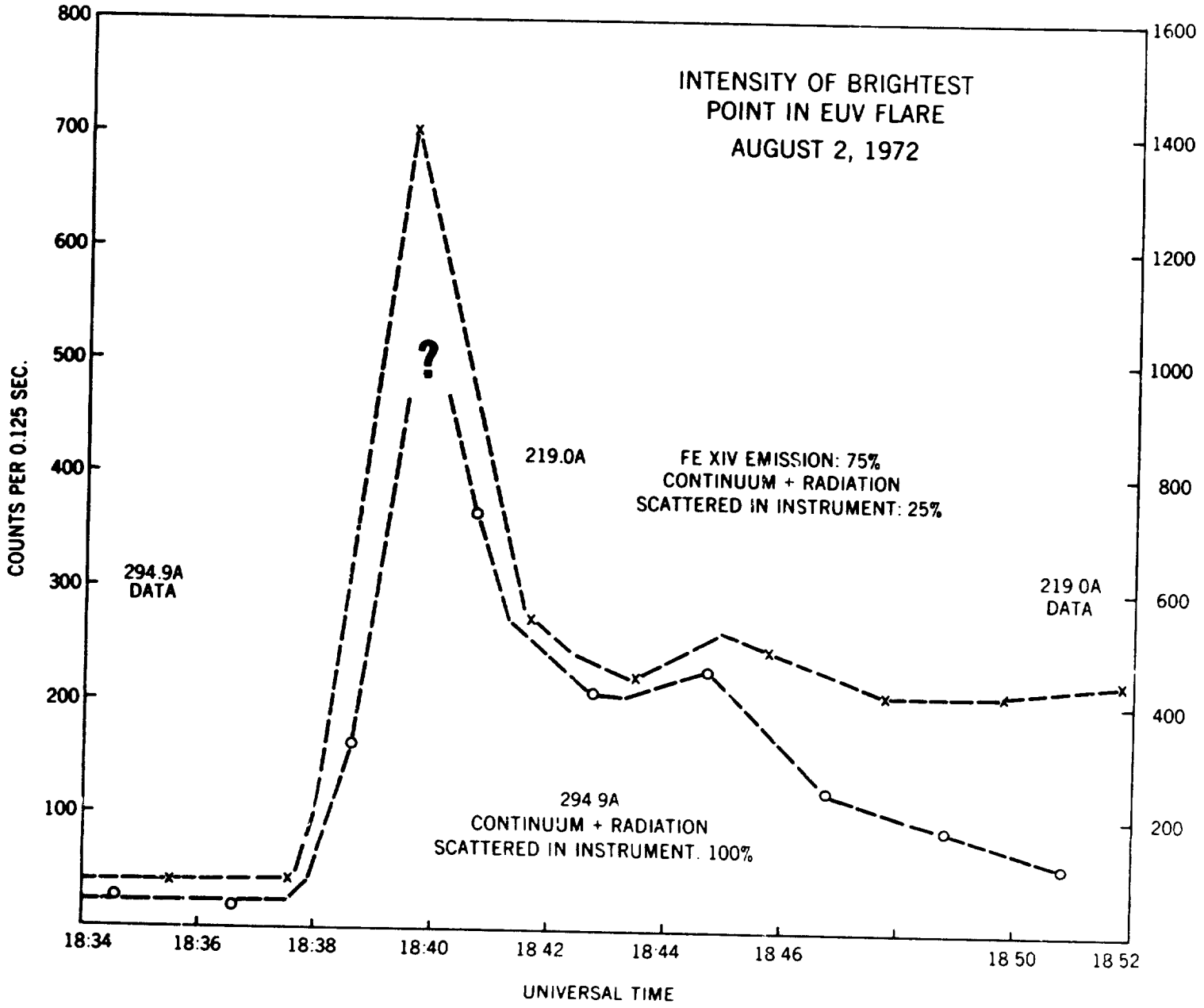
INTENSITY OF BRIGHTEST
POINT IN EUV FLARE
AUGUST 2, 1972
COUNTS PER 0.125 SEC.
800
700
600
500
400
300
200
100
1600
1400
1200
1000
800
600
400
200
?
219.0A
FE XIV EMISSION: 75%
CONTINUUM + RADIATION
SCATTERED IN INSTRUMENT: 25%
294.9A
DATA
219.0A
DATA
294.9A
CONTINUUM + RADIATION
SCATTERED IN INSTRUMENT: 100%
18:34
18:36
18:38
18:40
18 42
18:44
18 46
18 50
18 52
UNIVERSAL TIME

FIGURE 4

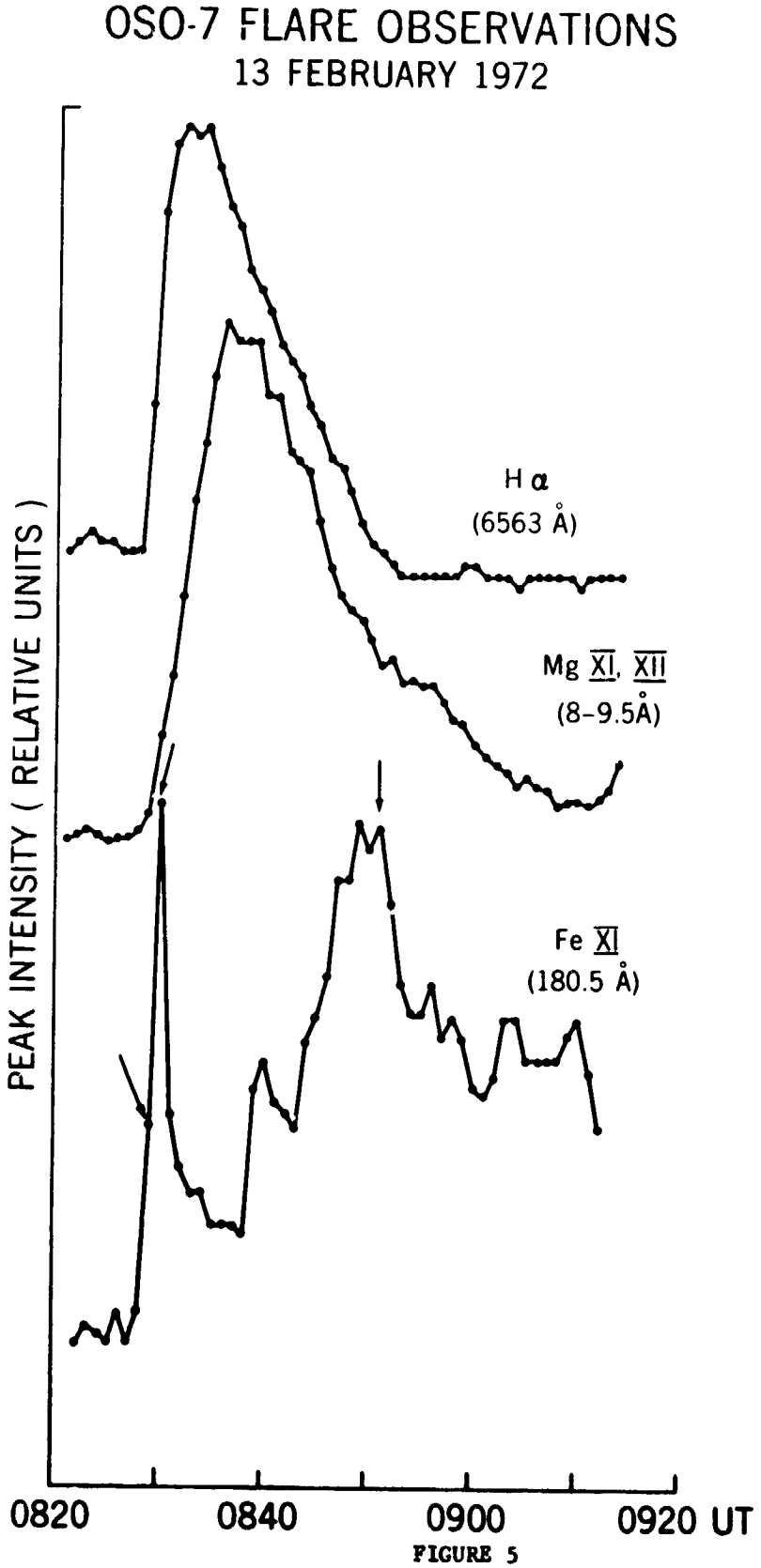

FIGURE 5

FLARE IMPULSIVE PHASE

13 FEB 1972 OSO-7

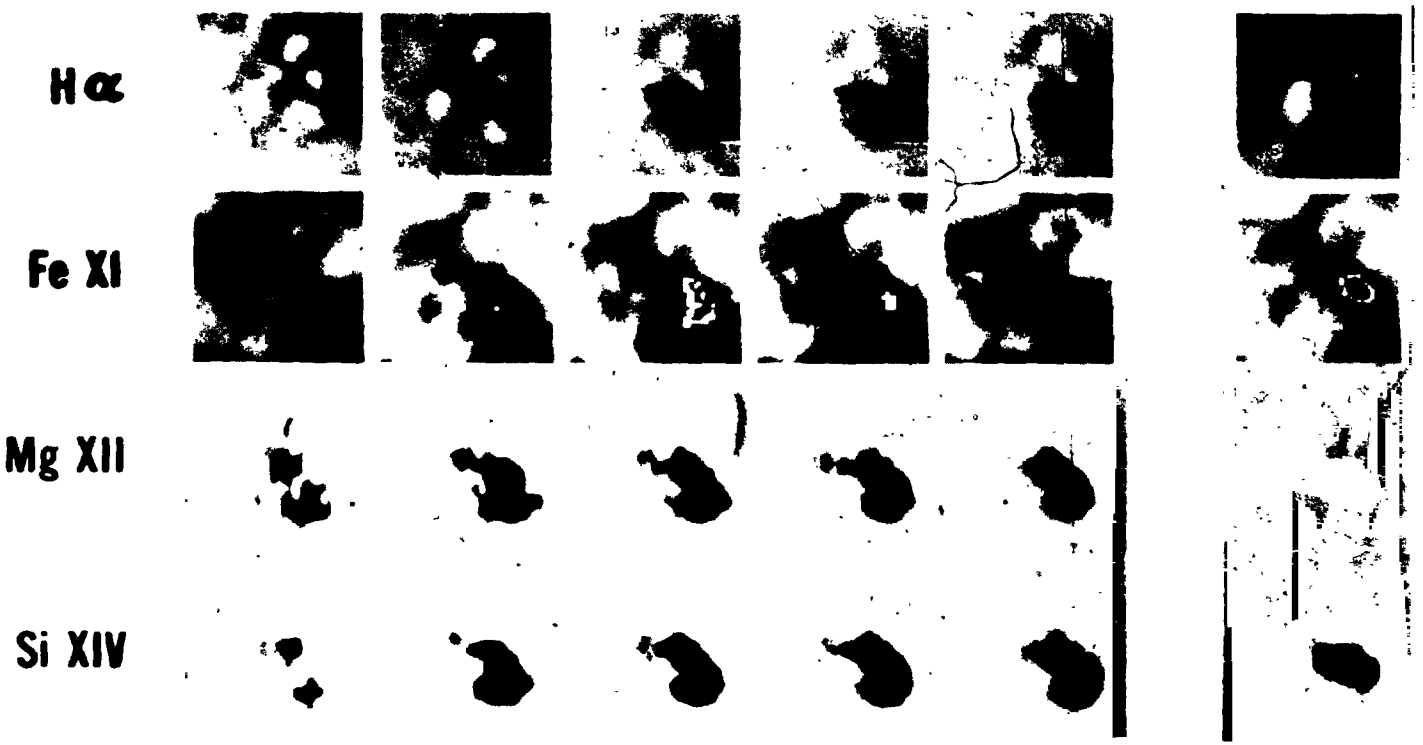

FIGURE 6

FLARE OBSERVATIONS ON JAN. 19, 1972
PRE-MAXIMUM EVOLUTION

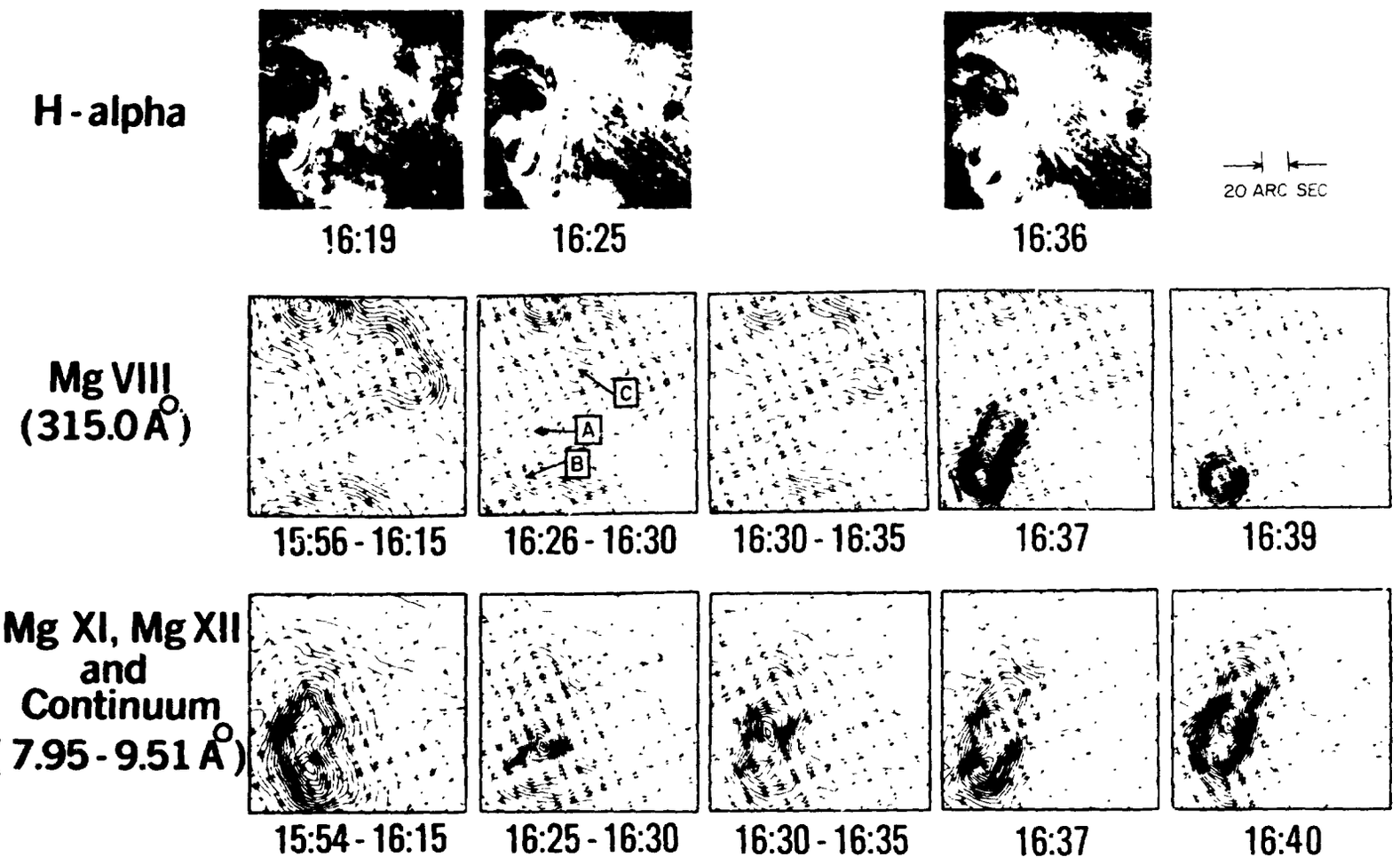

FIGURE 7

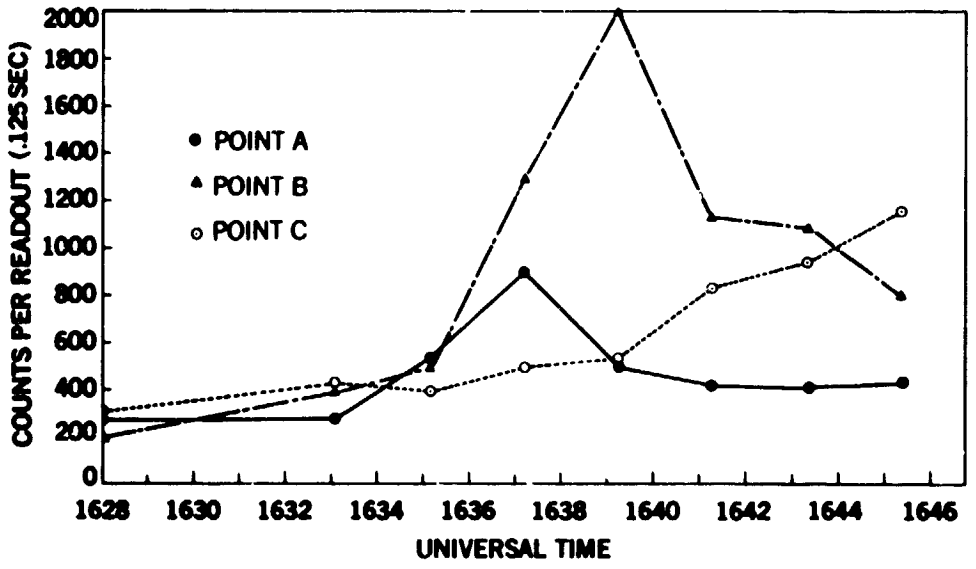
COUNTS PER READOUT (.125 SEC)
2000
1800
1600
1400
1200
1000
800
600
400
200
0
POINT A
POINT B
POINT C
1628
1630
1632
1634
1636
1638
1640
1642
1644
1646
UNIVERSAL TIME

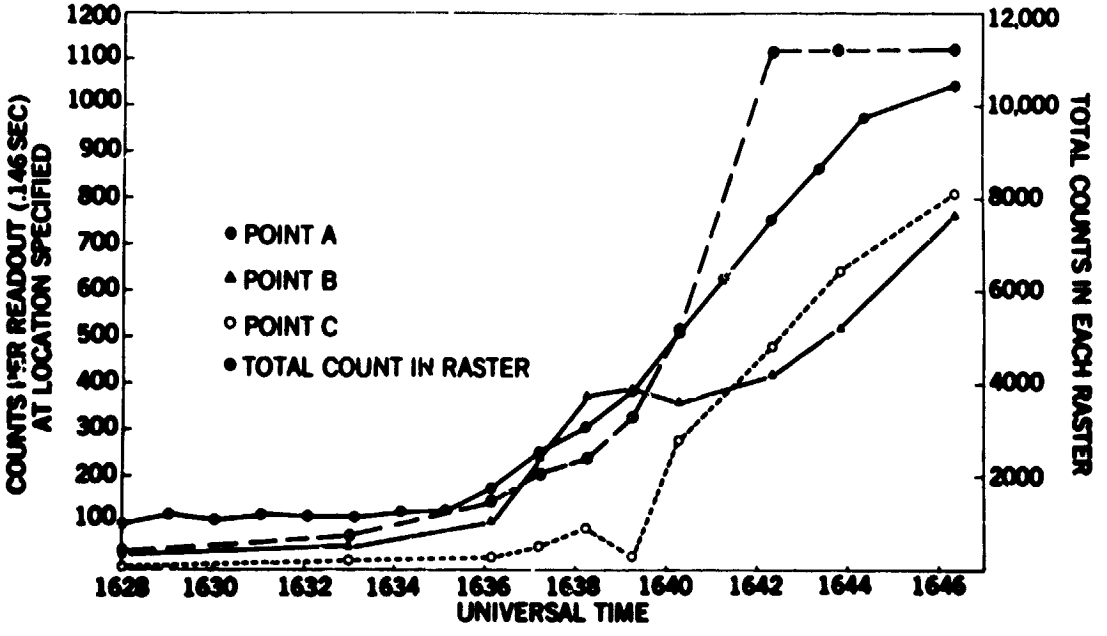
COUNTS PER READOUT (.146 SEC)
AT LOCATION SPECIFIED
1200
1100
1000
900
800
700
600
500
400
300
200
100
TOTAL COUNTS IN EACH RASTER
12,000
10,000
8000
6000
4000
2000
POINT A
POINT B
POINT C
TOTAL COUNT IN RASTER
1628
1630
1632
1634
1636
1638
1640
1642
1644
1646
UNIVERSAL TIME

FIGURE 8

(a)

(b)

(c)

Hα + 0.6 Å AT 1847:30 UT
(a) 294.9 Å AT 1846:49 UT
(b) 7.95-9.51 Å AT 1846:49 UT
(c) 1.90-2.07 Å AT 1845:47 UT

FIGURE 9

LIMB FLARE – POST MAXIMUM PHASE

February 10, 1972

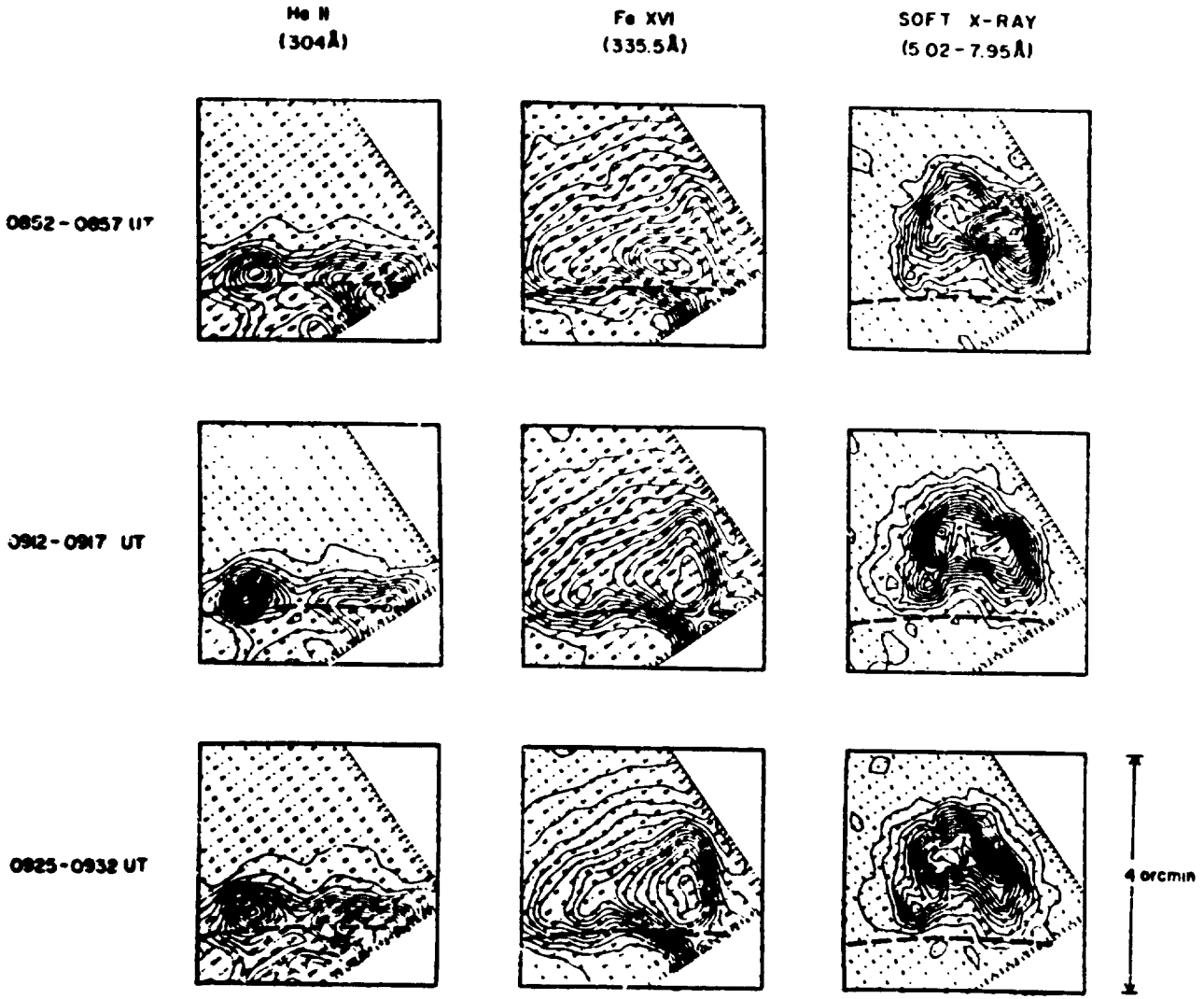

FIGURE 10

POST-FLARE LOOP SYSTEM
February 9, 1972, 0646 UT

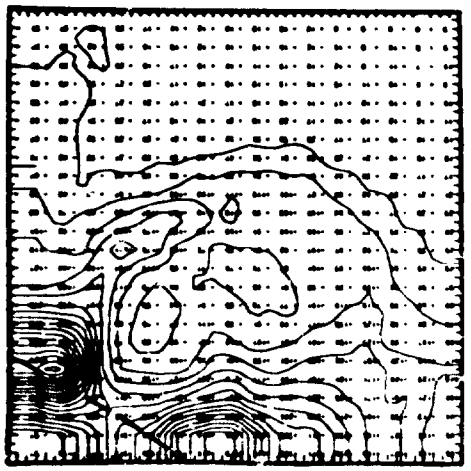

Mg VIII
(314.9Å)

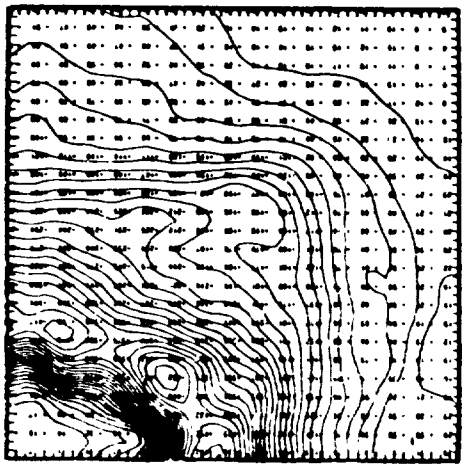

Fe XVI
(335.5Å)

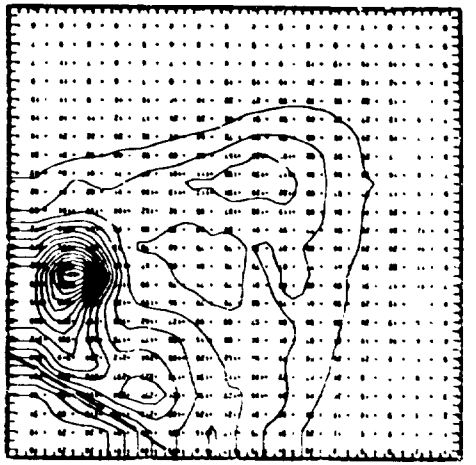

SOFT X-RAYS
(7.95-15 Å)

FIGURE 11